COMPONENT PART NOTICE

THIS PAPER IS A COMPONENT PART OF THE FOLLOWING COMPILATION REPORT:

(TITLE): Proceedings of the Conference on Improvement of Aerodynamic Performance through Boundary Layer Control and High Lift Systems Held at the Fluid Dynamics Panel Symposium in Brussels, Belgium on 21 23 May 1984.

(SOURCE): Advisory Group for Aerospace Research and Development, Neuilly-sur-Seine (France).

TO ORDER THE COMPLETE COMPILATION REPORT USE AD A147 396.

THE COMPONENT PART IS PROVIDED HERE TO ALLOW USERS ACCESS TO INDIVIDUALLY AUTHORED SECTIONS OF PROCEEDINGS, ANNALS, SYMPOSIA, ETC. HOWEVER, THE COMPONENT SHOULD BE CONSIDERED WITHIN THE CONTEXT OF THE OVERALL COMPILATION REPORT AND NOT AS A STAND-ALONE TECHNICAL REPORT.

THE FOLLOWING COMPONENT PART NUMBERS COMPRISE THE COMPILATION REPORT:

AD#:	TITLE:
P004 052	Recent Progress on Development and Understanding of High Lift Systems.
P004 053	Investigations into the Effects of Scale and Compressibility on Lift and Drag in the RAE 5m Pressurised Low-Speed Wind Tunnel.
P004 054	Recent Advances in Computational Methods to Solve the High-Lift Multi-Component Airfoil Problem.
P004 055	Inviscid Compressible Flow Past a Multi-Element Aerofoil.
P004 056	Design of an Airfoil Leading Edge Slat Using an Inverse Aerodynamic Calculation Method.
P004 057	Modelling Circulation Control by Blowing.
P004 058	Turbulent Bubbles behind Airfoils and Wings at High Angle of Attack.
P004 059	Aerodynamic Issues in the Design of High-Lift Systems for Transport Aircraft.
P004 060	An Update of the Canada/U.S.A. Augmentor-Wing Project.
P004 061	Aircraft Drag Reduction Technology.
P004 062	Theoretical Study of Boundary-Layer Control.
P004 063	Drag Reduction due to Boundary-Layer Control by Combined Blowing and Suction.
P004 064	Design Studies of Thick Laminar-Flow Airfoils for Low Speed Flight Employing Turbulent Boundary Layer Suction over the Rear Part.
P004 065	Technology Developments for Laminar Boundary Layer Control on Subsonic Transport Aircraft.
P004 066	Turbulent Drag Reduction Research.
P004 067	On the Relaxation of a Turbulent Boundary Layer after an Encounter with a Forward Facing Step.
P004 068	Full Scale Experiments into the Use of Large-Eddy-Breakup Devices for Drag Reduction on Aircraft.

COMPONENT PART NOTICE (CON'T)

AD#: P004 069 TITLE: Pneumatic Turbulators - A Device for Drag Reduction at Reynolds Numbers below 5, 000, 000.

P004 070 Active and Passive Shock/Boundary Layer Interaction Control on Supercritical Airfoils.

P004 071 Transonic Shock Interaction with a Tangentially-Injected Turbulent Boundary Layer.

DRAG REDUCTION DUE TO BOUNDARY-LAYER CONTROL BY COMBINED BLOWING AND SUCTION

by

J. Wiedemann, K. Gersten

University Bochum
Institut für Thermo- und Fluiddynamik
Postfach 10 21 48
D-4630 Bochum 1

use single quotes

SUMMARY

A boundary control system of combined blowing and suction is investigated. Blowing is applied in the front part of the body where the pressure gradient is favourable, whereas suction is applied in the rear part of the body where adverse pressure gradients exist. In order to avoid the "sink drag" the volume rate of suction should be equal or smaller than the blowing volume rate.

Theoretical investigations of laminar flows include optimization of the blowing velocity distribution as well as second-order boundary layer effects such as pressure drag and displacement effects on friction drag.

Experimental results (mean velocities and shear stresses) of turbulent boundary layers with very strong blowing velocities near the stagnation point of a circular cylinder are used as a basis of a simple prediction method. Experiments on a circular cylinder show considerable drag reductions due to the combined blowing and suction boundary layer control system.

1. INTRODUCTION

The drag of an immersed body can be determined by integrating the forces acting on the body surface. It consists of two parts: the pressure drag due to the pressure (normal) forces and the friction drag due to shear (tangential) forces.

In subsonic flow the pressure drag is originated mainly by boundary-layer separation. It is well-known that boundary-layer separation can be suppressed by boundary-layer control due to suction. The application of continuous suction on the body surface where usually boundary-layer separation may occur makes it possible to reduce the pressure drag of the body.

On the other hand, continuous blowing perpendicularly into the boundary-layer leads to a reduction of the wall shear stresses and hence to a reduction of the friction drag. Figure 1 shows the wall shear stress near the stagnation point of an immersed body in incompressible flow as a function of the blowing velocity. This result of Prandtl's boundary-layer theory leads to the conclusion, that the wall shear stress can be reduced to any value wanted if the blowing rate is chosen strong enough.

Reductions of both drag components, the pressure drag as well as the friction drag, could be achieved by a combination of boundary-layer control due to blowing and due to suction in such a way that blowing is applied on the surface area with accelerated flow where high wall shear stresses can be expected and suction on surface areas with decelerated flow with the danger of boundary-layer separation.

In this paper theoretical as well as experimental investigations will be discussed which refer to systems of boundary-layer control by combined blowing and suction. Laminar as well as turbulent flow will be considered.

2. LAMINAR FLOW

2.1. Prandtl's Boundary Layer Theory for Strong Blowing (and Suction)

When the boundary layer along a permeable body is controlled by blowing and/or suction, the solutions of Prandtl's boundary-layer equations lead to limiting solutions for very large blowing and/or suction rates. In Figure 1 the skin friction near the stagnation point in two-dimensional incompressible flow is shown as function of the blowing velocity v_w (negative v_w corresponds to suction). There are two asymptotes for the skin-friction curve corresponding to the two limiting solutions of the boundary layer equations. In the limit of strong suction the skin friction increases with growing suction velocity. The skin friction is equivalent to the so-called "sink drag" due to momentum loss by suction. In order to avoid this sink drag the air sucted in has to be blown out again at a proper area. This leads to another limiting solution for large blowing velocity, sometimes called the "blowhard problem", see [1]. As Figure 1 shows, in this limit the skin friction is inversely proportional to the blowing velocity v_w, in other words, it can be reduced as much as desired, if the blowing velocity v_w is chosen large enough. For the given outer-flow velocity distribution $U(x)$ and the blowing velocity distribution $v_w(x)$ the wall shear stress is given by the simple formula:

$$\tau_w(x) = \frac{\rho \nu U(x)}{v_w(x)} \frac{dU}{dx} \tag{1}$$

This formula, originally derived for blowing ($v_w > 0$ and $dU/dx > 0$) can also be applied for suction, if the combination $(1/v_w(x))(dU/dx)$ stays positive, i.e. when suction is used at adverse pressure gradients ($v_w < 0$, $dU/dx < 0$). As the formula shows the wall shear stress is inversely proportional to the blowing velocity $v_w(x)$. In this limit of strong blowing the flow field has a three-layer structure as shown in Figure 2 for the example of a circular cylinder with $v_w \sim \cos \phi$, i.e. when blowing is applied on the front part of the cylinder and suction on the rear part of the cylinder. The viscosity is not essential for satisfying the no-slip condition at the wall and plays a role only in a thin free shear layer along the dividing streamline detached from the wall.

The drag coefficient of the circular cylinder (d: diameter; b: span; R: radius; $Re = U_\infty d/\nu$) is in this limit

$$c_D = \frac{D}{\frac{\rho}{2} U_\infty^2 \, b \, d} = \frac{8 \pi}{c_M \sqrt{Re}} \tag{2}$$

where

$$\frac{v_w(x)}{U_\infty} \sqrt{Re} = c_M \cos \frac{x}{R} \quad . \tag{3}$$

The mass-transfer coefficient c_M is connected with the volume rate coefficient

$$c_Q = \frac{Q}{U_\infty \, b \, d} \tag{4}$$

by

$$c_M = c_Q \sqrt{Re} \tag{5}$$

where Q is the volume rate of the recirculating flow inside the dividing streamline (see Figure 2).

In Figure 3 the drag reduction of a circular cylinder by two different boundary-layer control systems is shown for the Reynolds number $Re = U_\infty d/\nu = 4 \cdot 10^4$. Curve I refers to the combination of blowing and suction according to Eq. (3), whereas curve II corresponds to the case of homogeneous suction with the total suction rate Q. The asymptote of curve I, given by Eq. (2), shows clearly that the drag can become as small as desired if the circulating flow rate is large enough. On the contrary, curve II shows a drag reduction down to a value of $c_D \approx 0.2$, but further suction will increase the drag due to the sink drag, see also Figure 1. The comparison shows very clearly that the system of combined blowing and suction is much more effective than the system of homogeneous suction.

For bodies other than the circular cylinder the Eqs. (2) and (5) will also be valid with just different coefficients. For a symmetrical Joukowsky airfoil (4.4 % relative thickness) the drag coefficient as function of the volume rate coefficient is shown in Figure 4. In this example the distribution of the blowing velocity v_w was chosen $v_w \sim dU/dx$ in order to make sure that the combination $(1/v_w)(dU/dx)$ is always positive. As a consequence, the blowing rate Q_{Blow} is larger than the suction rate Q_{Suc}, namely $Q_{Blow} = 9.1 \, Q_{Suc}$. The excess of blowing rate is equivalent to a thrust of the airfoil similar to the sink drag in the case of suction. But Prandtl's boundary-layer theory is not able to cover this thrust effect, which, as will be shown later, is a higher-order boundary-layer effect.

2.2. Optimization

For a given body geometry and a given velocity distribution U(x) the following optimization problem can be formulated:

> An optimal distribution $v_w(x)$ has to be found such that the drag becomes a minimum under the additional condition of equal blowing and suction volume rates.

Figure 5 shows the result for such an optimization of the circular cylinder. Curves I correspond to the case shown in Figure 2 and given by Eq. (2). Due to optimizing the v_w-distribution (curves II) the drag could be reduced by 44 % from $c_D \, c_Q \, Re = 25$ down to $c_D \, c_Q \, Re = 14$.

A similar optimization of the symmetrical Joukowsky airfoil (4.4 % relative thickness) led to the minimum value $c_D \, c_Q \, Re = 1.0$. Each body has its minimum value $c_D \, c_Q \, Re$ depending on the velocity distribution U(x).

2.3. Second-Order Boundary-Layer Theory.

When in the system of combined blowing and suction the blowing rate is larger than the suction rate, a negative drag, i.e. thrust, is produced. This force against the oncoming

flow direction must be a pressure force. This, however, cannot be predicted by Prandtl's boundary layer theory. This thrust due to blowing is a second-order boundary layer effect. Second-order boundary layer theory will also yield information about the displacement effects of the fairly thick boundary layers due to blowing.

The second-order boundary-layer effects for the circular cylinder ($v_w \sim \cos\phi$, see Figure 2) have been investigated in [2]. The drag formula, Eq. (2), has been extended to

$$c_D = \frac{8\pi}{c_M\sqrt{Re}} + \frac{2\pi^2}{Re} \qquad (6)$$

It is worth mentioning, that the second-order term is independent of c_M.

Figure 6 shows the second-order effects on the drag of the Joukowsky airfoil ($v_w \sim dU/dx$, see Figure 4) at Reynolds number $Re = U_\infty c/\nu \approx 10^4$ (c = chord length of airfoil). The blowing rate $c_{Q\,Blow}$ is larger than the suction rate $c_{Q\,Suc}$, therefore thrust due to blowing occurs, $c_D = -1.78\, c_{Q\,Blow}$. As in the example of the circular cylinder an additional friction drag due to second-order effects (displacement effects) exists, which reaches a finite value of $c_D \approx 0.0052$ (independent of $c_{Q\,Blow}$) for infinitely large blowing rates. Contrary to the circular-cylinder example where second-order effects on drag were only friction drag, here also a pressure drag (curve IIb) exists, which unfortunately has the same order of magnitude as the friction-drag reduction due to blowing.

3. TURBULENT FLOW

3.1. Experiments of the Flow Field Near Stagnation Point

So far, laminar flow was assumed. But in the area where blowing is applied, turbulent flow has to be expected, because blowing has a strong destabilizing effect on the boundary layer. Therefore, detailed measurements of the flow characteristics (mean velocities, turbulence intensities, turbulent shear stresses) within the boundary layer with blowing have been undertaken by using Laser-Doppler anemometry, [4]. The experiments have been carried out at the stagnation point area of a porous circular cylinder (see Figure 2) with extremely large blowing rates (up to $v_w/U_\infty = 0.18$) which have not yet been reported in the literature.

Figures 7 and 8 show the mean velocities and the turbulent shear stresses at different positions over the front part of the circular cylinder. Turbulent boundary layers along impermeable walls have usually a two-layer structure with the "wall" layer and the "defect" layer, where the friction velocity $u_\tau = \sqrt{\tau_w/\rho}$ is the characteristic velocity.

Turbulent boundary layers with strong blowing still have the two-layer structure, but with a few important differences.
Firstly, the basic characteristic velocity is

$$u_{\tau\,max} = \sqrt{\frac{\tau_{max}}{\rho}} \qquad (7)$$

i.e. based on the maximum shear stress τ_{max} within the boundary layer (see Figure 8) rather than based on the wall stress τ_w.
Secondly, the boundary layer thickness is growing with the blowing velocity, but the defect layer is growing relatively faster than the wall layer, in other words, the defect layer plays an increasing role compared to the wall layer when the blowing rate is increasing.

As a consequence, all velocity distributions shown in Figure 7, will approximately collapse into one universal curve (except close to the wall) if represented as defect laws according to

$$\frac{U - u}{u_{\tau\,max}} = g\left(\frac{y}{\delta}\right) \quad , \qquad (8)$$

see for details [4]. This law can be interpreted as an extension of the law of the wake by McQuaid [5]. The function $g(y/\delta)$ is identical with the one found by McQuaid for blowing rates up to $v_w/U = 0.008$. It should be mentioned that McQuaid used a characterstic velocity different from $u_{\tau\,max}$. In [4] however it is shown by asymptotic arguments why $u_{\tau\,max}$ is the proper velocity scale.

In Figure 9 the experimental results are shown as defect laws according to Eq. (8) and compared with McQuaid's defect law. Particularly the results for $\phi = 30^\circ$ show that the defect law covers most of the boundary layer for cases of strong blowing.

3.2. Prediction of Turbulent Boundary Layers with Strong Blowing.

Turbulent boundary layers with strong blowing are very well represented by the defect layer governed by Eq. (8) . This result was used as a basis for a simple prediction method of such boundary layers. The following equations have been applied:

a) Momentum integral equation for the defect layer (neglecting the small wall shear stress):

$$\delta_1 \, U \, \frac{dU}{dx} + \frac{d}{dx} \, (\delta_2 \, U^2) = v_w \, U \, . \tag{9}$$

b) Velocity distribution according to defect law of Eq. (8):

$$\frac{u}{U} = 1 - \frac{u_{\tau \, max}}{U} \, g(\frac{y}{\delta}) \, . \tag{10}$$

This leads to

$$\frac{\delta_1}{\delta} = f_1(\frac{u_{\tau \, max}}{U}) \quad , \qquad \frac{\delta_2}{\delta} = f_2(\frac{u_{\tau \, max}}{U}) \, . \tag{11}$$

There are two unknowns $\delta(x)$ and $u_{\tau \, max}(x)$ for given $U(x)$ and $v_w(x)$. In addition to Eq. (9) an entrainment relationship has been used:

$$\frac{dQ}{dx} = \frac{d}{dx} \, [U \, (\delta - \delta_1)] = v_E + v_w \tag{12}$$

where

$$\frac{v_E}{u_{\tau \, max}} = c_E \approx 0.08 \, , \tag{13}$$

a value typical of entrainments of wakes.
The Eqs. (9) to (13) are a complete set to predict $\delta(x)$ and $u_{\tau max}(x)$ for given $U(x)$ and $v_w(x)$. Figure 10 shows the results of such a prediction and the comparison with the experiments described in Chapter 3.1. The wall shear stress depicted in Figure 10c has been determined from $u_{\tau \, max}(x)$ by a simple estimation given in [4].

The prediction method presented here can be used for a good estimation of the behaviour of turbulent boundary layers with very strong blowing.

4. EXPERIMENTS ON DRAG REDUCTION OF A CIRCULAR CYLINDER

The combination of boundary layer control by blowing and suction has been applied to a circular cylinder in incompressible flow. In Figure 11 a typical arrangement is shown. The front quarter of the cylinder periphery was used for blowing, whereas the rest of the periphery was used for suction. The suction velocity was one third of the blowing velocity to make sure that the net volume rate was equal to zero. Typical results for the pressure distributions at $Re = 9 \cdot 10^4$ are shown in Figure 12. Due to boundary-layer control the pressure drag could be reduced considerably from $c_D = 1.04$ without control down to $c_D = 0.52$ for $v_{w \, suc}/U_\infty = 0.03$. From the comparison with the pressure distribution of potential theory it can be concluded that even better results might be possible by further refinement of the combined boundary layer control system.

5. REFERENCES

[1]: J. D. Cole, J. Aroesty: The blowhard problem - Inviscid flow with surface injection. Int. J. Heat Mass Transfer Vol. II, 1968, 1167-1183.

[2]: K. Gersten: Second-order boundary-layer effects for large injection or suction. In: U. Müller, K.G. Roesner, B. Schmidt (Editors), Recent Developments in Theoretical and Experimental Fluid Mechanics. Springer, Berlin 1979, pp. 446-456.

[3]: K. Gersten, J. Wiedemann: Widerstandsverminderung umströmter Körper durch kombiniertes Ausblasen und Absaugen an der Wand. Forschungsbericht Nr. 3103 des Landes Nordrhein-Westfalen, Westdeutscher Verlag, Opladen 1982.

[4]: J. Wiedemann: Der Einfluß von Ausblasen und Absaugen an durchlässigen Wänden auf Strömungen bei großen Reynoldszahlen, Doctoral Thesis, University of Bochum, 1983.

[5]: J. McQuaid: A velocity defect relationship for the outer part of equilibrium and near-equilibrium turbulent boundary layers, ARC CP No. 885, 1965.

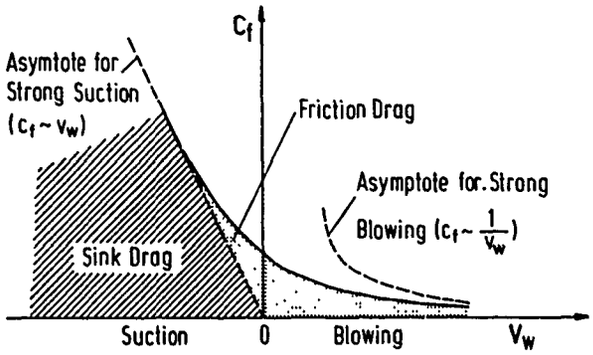

Figure 1: Skin Friction near the Stagnation Point in Two-dimensional Incompressible Flow

Figure 2: Flow past a Circular Cylinder
Blowing in the Front Part
Suction in the Rearward Part

Three Layer Flow
I : Inviscid Outer Flow (Potential Flow)
II : Free Shear Layer
III: Inviscid Inner Layer with Vorticity

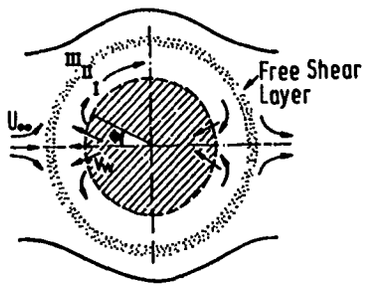

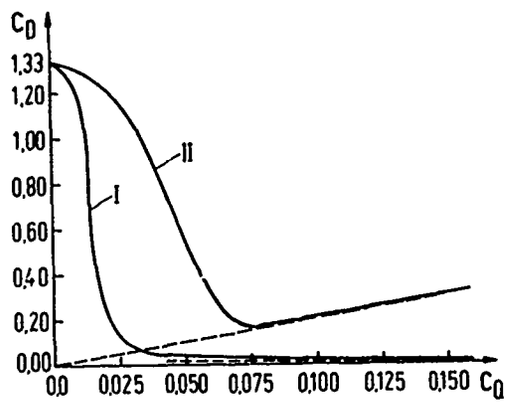

Figure 3: Drag Reduction of a Circular Cylinder by Two Different Boundary-Layer Control Systems.
$Re = 4 \cdot 10^4$

I : Combined Blowing and Suction $v_W \sim \cos \phi$,
c_Q : Volume Rate Coefficient of Recirculating Flow. Asymptote: $c_D = 6.25 \cdot 10^{-4}/c_Q$

II: Homogeneous Suction, v_W = const.
c_Q : Suction Coefficient
Asymptote: $c_D = 2 \cdot c_Q$ (Sink Drag)

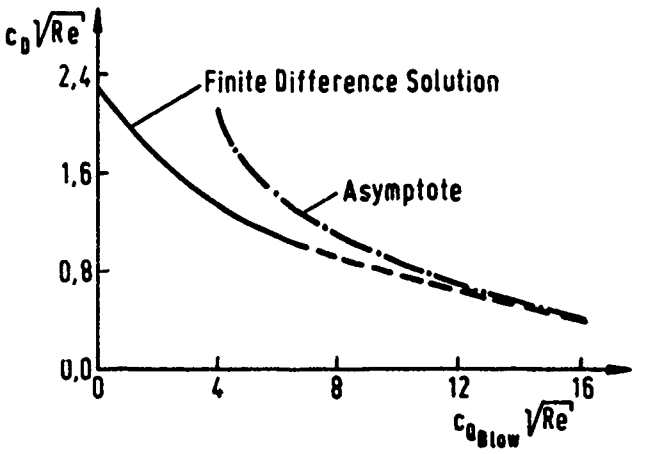

Figure 4: Friction Drag of a Symmetrical Joukowsky Airfoil (4,4 % Relative Thickness) as Function of the Blowing Rate. $v_W \sim dU/dx$, $Q_{Blow} = 9.1\ Q_{Suc}$
Asymptote: $c_D\sqrt{Re} = 8.8/c_{Q\,Blow}\sqrt{Re}$

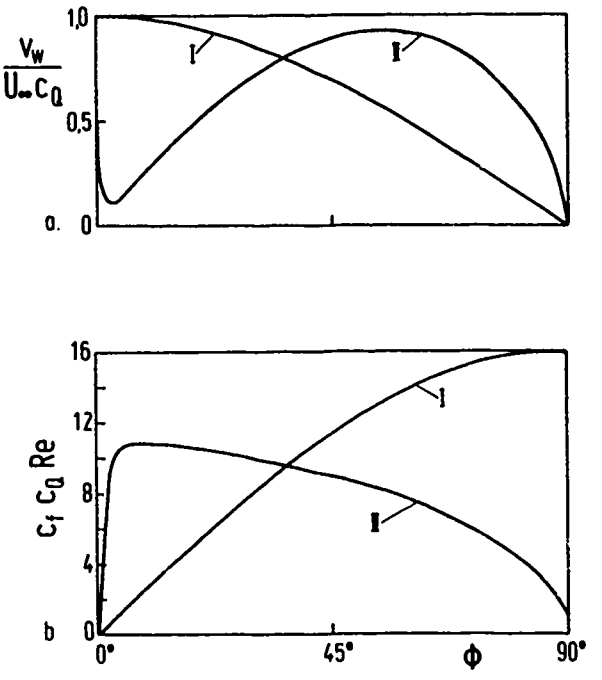

Figure 5: Effect of Distribution of Blowing-Suction Velocity on Drag Reduction. Circular Cylinder in Laminar Flow for the Limit of Strong Blowing and Suction.
a. Blowing-Suction Velocity Distribution
(The same blowing rate for both curves)
b. Shear Stress Distribution

I : $v_W \sim \cos\phi$, $c_D \cdot c_Q \cdot Re = 25$

II: Optimal v_W-Distribution, $c_D \cdot c_Q \cdot Re = 14$

c_Q : Volume Rate of Recirculating Flow

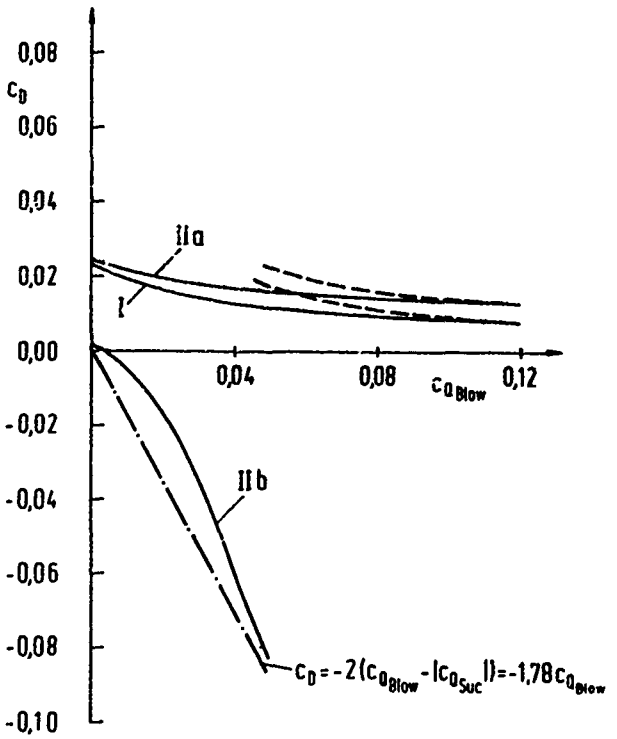

Figure 6: Drag Reduction of Joukowsky Airfoil by Combined Blowing and Suction.

I : Prandtl's (first order) Boundary-Layer Theory.
Asymptote for Friction Drag: $c_D = 9.1 \cdot 10^{-4}/c_{Q\,Blow}$
$c_{Q\,Blow}$: Blowing Rate Coefficient = 9.1 $c_{Q\,Suc}$

II: Second Order Boundary-Layer Theory.
IIa: Friction Drag
IIb: Pressure Drag
----- Thrust due to Blowing, $c_D = -1.78\ c_{Q\,Blow}$

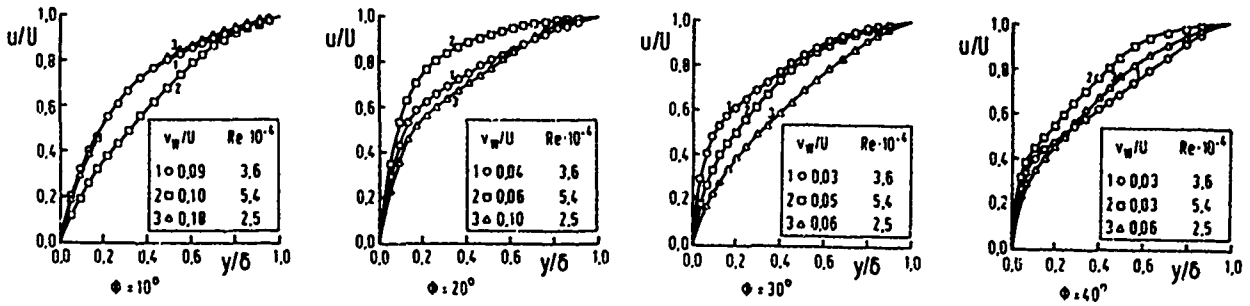

Figure 7: Mean Velocities in the Boundary Layer in the Stagnation Region of a Circular Cylinder with Strong Blowing (LDA Measurements) Re = $U_\infty d/\nu$, U = U(x) : Local Outer Flow Velocity.

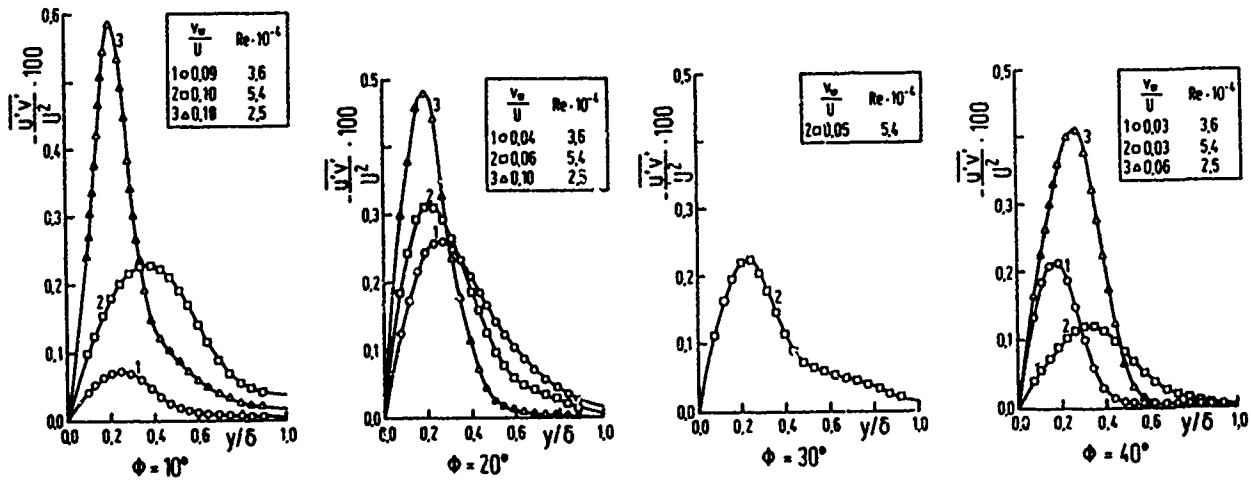

Figure 8: Turbulent Shear Stresses in the Boundary Layer with Strong Blowing, See Figure 7.

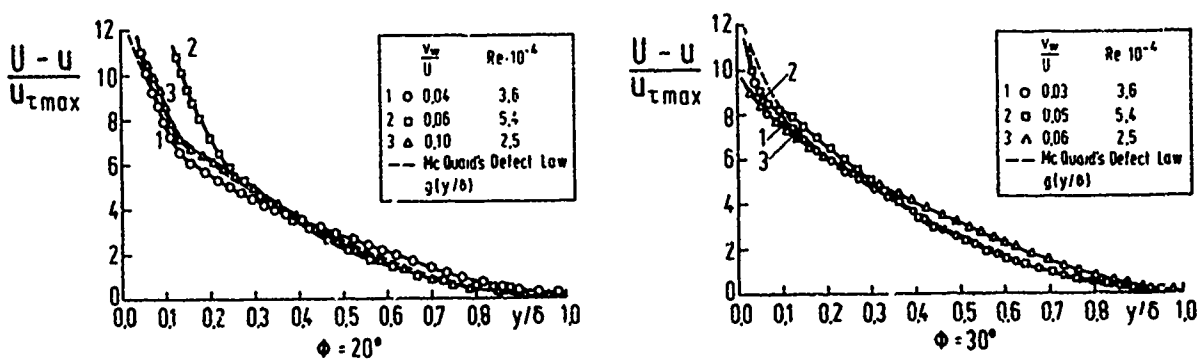

Figure 9: Defect Law in the Boundary Layer with Strong Blowing.
See Figures 7 and 8.

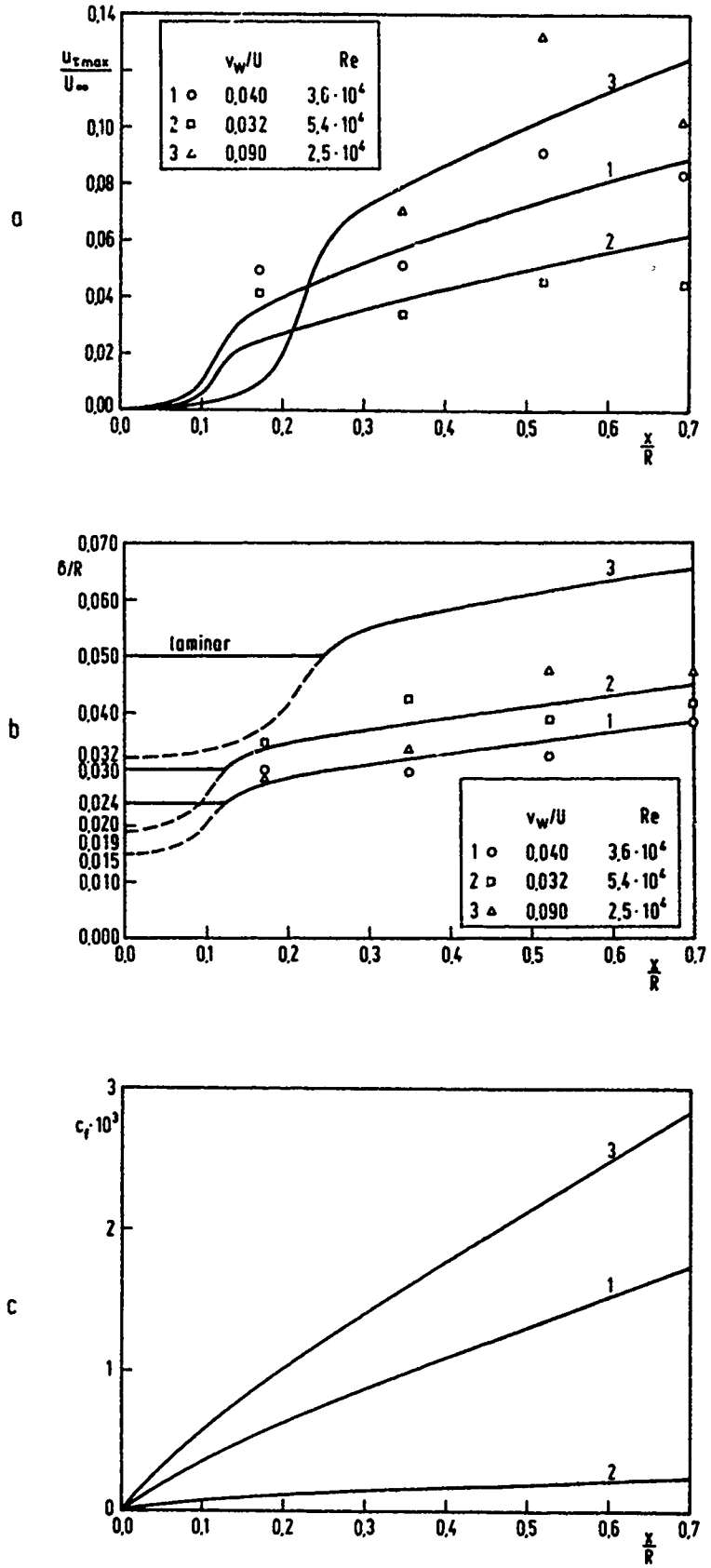

Figure 10: Prediction of Maximum Shear Stress $u_{\tau\,max}$, Boundary Layer Thickness δ, and Skin Friction Coefficient c_f in the Boundary Layer in the Stagnation Region. Comparison of Theory and Experiment.

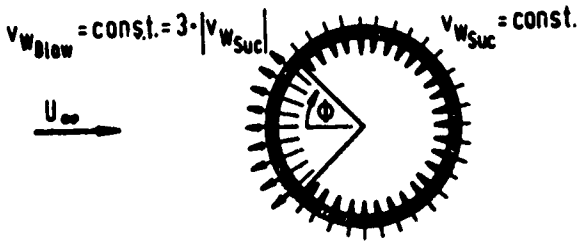

Figure 11: System of Combined Blowing and Suction Applied to a Circular Cylinder, $Q_{Blow} = Q_{Suc}$
$v_{W\,Blow} = 3\ v_{W\,Suc}$

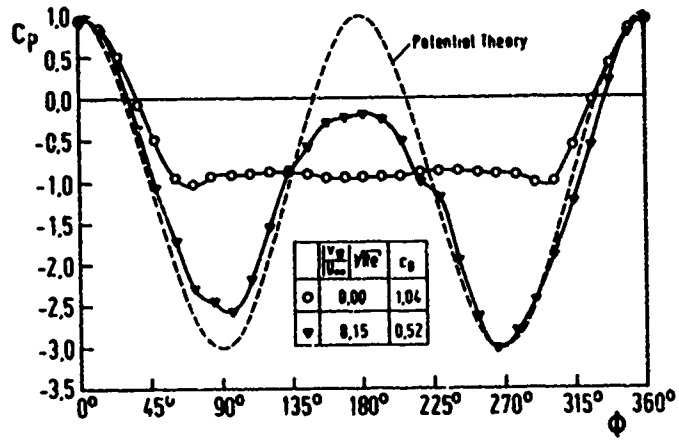

Figure 12: Pressure Distribution on a Circular Cylinder at Re = $9 \cdot 10^4$, $c_p = 2(p-p_\infty)/\rho\ U_\infty^2$.

o No Boundary Layer Control
Pressure Drag: $c_D = 1.04$

▽ Combined Blowing and Suction Boundary Layer Control According to Figure 11, $v_{W\,Suc}/U_\infty = 0.03$
Pressure Drag: $c_D = 0.52$